Trans Indian Inst Met (2018) 71(10):2497–2504
https://doi.org/10.1007/s12666-018-1380-2

TECHNICAL PAPER

Effect of Cold Rolling Parameters on Bond Strength of Ti Particle Embedded Al Strips

Zohreh Yazdani[1] · Mohammad Reza Toroghinejad[1] · Hossein Edris[1] · Alfonso H. W. Ngan[2]

Received: 15 February 2018 / Accepted: 9 July 2018 / Published online: 21 July 2018

Abstract Bond strength of cold roll bonded Al layers with and without Ti particles was studied. The effect of particle's content that was placed between aluminium sheets and rolling reduction on weld efficiency and bonding was studied. Peel test was used to measure the adhesive strength between the bonded Al strips. The weld efficiency η of the roll bonding process was calculated. The results showed that the weld efficiency in the presence of Ti is lower than that in the absence of Ti. The surface conditions of the peeled surfaces were inspected by scanning electron microscopy. It could be concluded that by enhancing the rolling reduction up to 70%, the bonded area on the interface is increased and bonds with higher strength are produced. However, the addition of Ti particles leads to reduction of the bonded area and bond strength. Also, presence of Ti powders up to 0.5 wt%, lead to the increase of threshold deformation to 45%.

Keywords Bond strength · Roll bonding · Al sheet · Ti particles

✉ Zohreh Yazdani
z.yazdani@ma.iut.ac.ir

Mohammad Reza Toroghinejad
toroghi@cc.iut.ac.ir

Hossein Edris
h-edris@cc.iut.ac.ir

Alfonso H. W. Ngan
hwngan@hku.hk

[1] Department of Materials Engineering, Isfahan University of Technology, Isfahan 84156-83111, Iran

[2] Department of Mechanical Engineering, The University of Hong Kong, Pokfulam Road, Hong Kong, China

1 Introduction

Cold roll bonding (CRB) has become an attractive manufacturing process to fabricate composite material sheets. CRB is a solid phase method of bonding that is created by plastic deformation of bonded metals. In this process, roll pressure causes breaking of oxide films and formation of cracks. Then bonding can occur by extruding material through cracks [1–5]. Most of materials can be joined together by CRB, specialty alloys cannot be bonded by other traditional bonding techniques [6]. It is easy to get enough bond strength by CRB for pure metals like pure Al or Cu. But for other alloys like precipitation hardened Al alloys, for obtaining strong bonding, rolling temperature is required to increase [7]. According to previous studies, there are many factors that influence roll bonding quality such as thickness reduction [6, 8–19], temperature of rolling [17], post annealing [18], speed of roll bonding [16, 19] and the presence of particles between metal strips [20, 21]. The effects of adding ceramic powders between the bonding strips have also been investigated by a number of research groups. For example, TiH_2 powder has been placed between Al strips to create Al foams but this results in lower bond strength for Al [20]. Another research by Lu et al. [21] showed that adding SiO_2 powder to Al strips, forms Al matrix composite and increases the bond strength. Metallic multilayer composites have attracted much attention due to the considerable advantages presented by their mechanical, magnetic, and electrical properties [22]. Therefore, the effects of presence of Ti powders between Al strips during rolling on the bond strength is an interesting aspect to study. Then Al/Ti panel start to fabricate a composite with Ti-aluminide intermetallic compound [23].

So, the purpose of this article is fabrication of Al sheet/Ti powders/Al sheet sandwich by cold roll bonding and then to study the effects of the amount of the particles, as well as thickness reduction on the bond strength.

2 Experimental Procedure

Commercially pure (AA 1100) aluminium sheets were cut into 100 × 50 × 1 mm^3 strips parallel to the sheet rolling direction, and then annealed at 370 °C for 1 h, under laboratory conditions, without the provision of protective environments. Then, samples were scratch brushed by a brush made of stainless steel with wire diameter of 0.25 mm, according to recommendations from previous studies to achieve roll bonding [24].

The roughness profile meter (SM7) was used for determining surface roughness based on ASTM-D7127 standard. Roughness test was repeated for 10 random points. The mean roughness values of the samples before and after brushing were 0.5 μm and 3 μm, respectively.

99.9% pure Ti particles, supplied by Merck (Fig. 1a, b), were prepared to apply between two Al strips before the CRB process. To achieve powders with small size and narrow range of size, ball milling was used. Milling was made in a Retsch PM100 planetary ball mill using 5 balls in the atmosphere of argon for 7 h. The ball to powder weight ratio and speed of container were 10:1 and 500 rpm, respectively. Morphology of Ti particles after milling is shown in Fig. 1c, d. The particle size distribution of Ti was determined by digital image processing (DIP) technique (Fig. 2). After milling, average size of Ti particles decreased from 45 to 0.8 μm. An ethanol-based suspension was used for applying Ti powders with good distribution on aluminium sheets. As shown in Fig. 3, after brushing, suspension was sprayed uniformly on the surface. Then, aluminium sheets with and without Ti powders were put on each other, stacked, and both ends were riveted. The stacked strips were buttoned at both end by steel wire and were roll bonded as soon as surface preparation was finished.

The amount of Ti powder varied between 0.3 and 0.5 wt%. A laboratory rolling mill with no lubrication was used for roll bonding. Rolling was carried out with rolling speed of 4 m/min to rolling reductions of 40, 50, 60 and 70%.

The applied cold roll bonding process for aluminium sheets with Ti powder particles is shown schematically in Fig. 4. For comparison purposes, CRB was also performed on Al strips without the addition of Ti powder.

Peel tests of the bonded samples were carried out by the Hounsfield tensile testing machine (model H50KS) at a crosshead speed of 20 mm/min. The ASTM standard D1876-01 was applied for the measurement of the bond

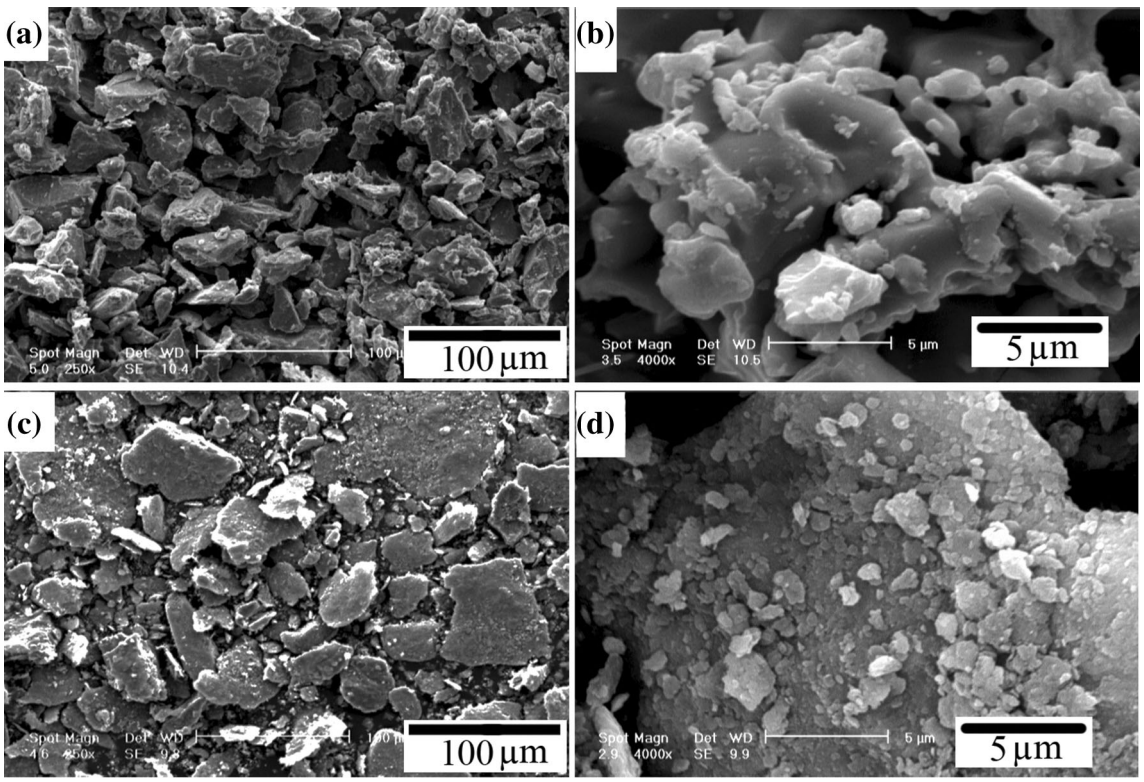

Fig. 1 SEM micrograph of the Ti particles

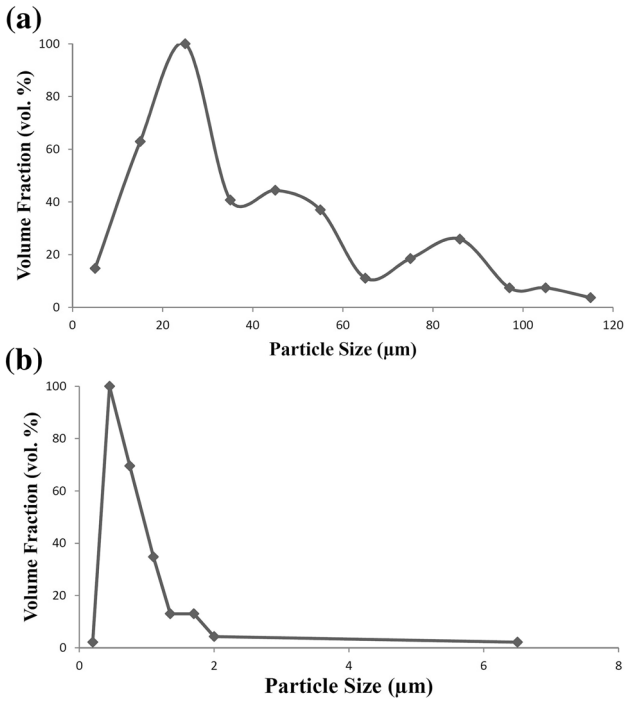

Fig. 2 Image analysis of the Ti particles: **a** before milling and **b** after milling

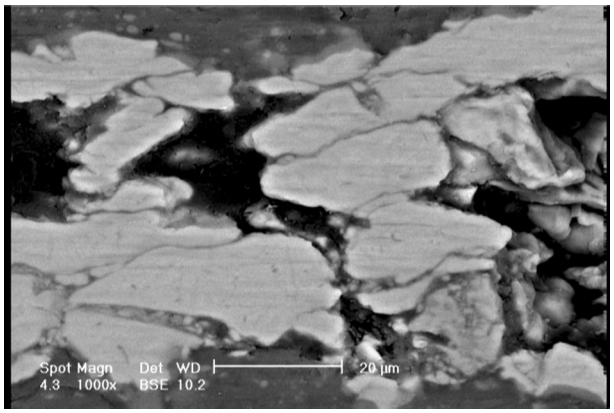

Fig. 3 Image of applying Ti powders on Al-1100 sheet

strength of lamination sheets. The average peel strength was estimated as [25]

$$\text{Average Peel Strength} = \frac{\text{Average Peel Force}}{\text{Bond Width}}\left(\frac{\text{N}}{\text{mm}}\right) \quad (1)$$

Three peel tests were performed for each sample and the mean peel strength were calculated. A PHILIPS XL30 scanning electron microscope (SEM) was used to evaluate fractured surfaces of the aluminium sheets after the peel tests.

The weld efficiency η of the roll bonding process, defined as

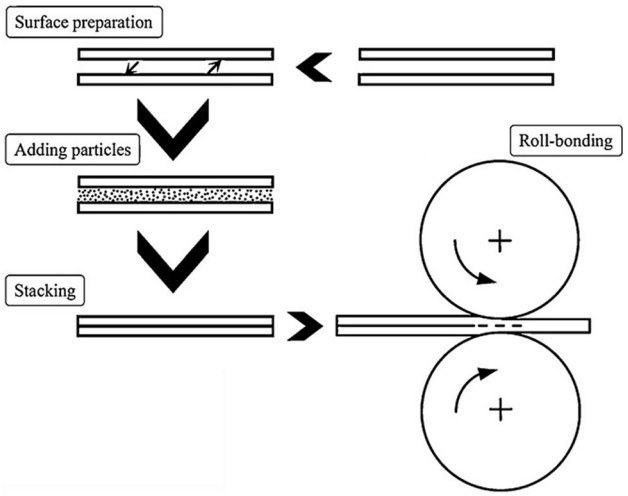

Fig. 4 Schematic illustration of cold roll bonding procedure

$$\eta = S_w/S_m \quad (2)$$

where S_w and S_m are the strengths of the weld and the base metal respectively, was also calculated. Following Madaah-Hosseini and Kokabi [26], the base metal strength S_m was assumed to obey a simple plastic rule

$$S_m = K\varepsilon^n \quad (3)$$

where K is the strength coefficient, n is the strain hardening exponent, which have been obtained for the investigated alloy by tensile testing and the plastic strain is given as

$$\varepsilon = \frac{2}{\sqrt{3}}\ln\left(\frac{1}{1-R_f}\right) \quad (4)$$

with R_f being the final rolling reduction. The weld strength S_w is estimated from the peel tests as

$$S_w = \frac{F_w}{A_w} \quad (5)$$

where F_w is the maximum force for break down recorded from the peel test, and A_w is the effective load-bearing area. With Eqs. (3) (4) and (5), Eq. (2) becomes

$$\eta = \frac{F_w}{A_w K}\left[\frac{2}{\sqrt{3}}\ln\left(\frac{1}{1-R_f}\right)\right]^{-n} \quad (6)$$

To determine A_w, the condition for $\eta = 1$ has been used, at which the failure of the base metal determines the breakage of the weld. Denoting the critical rolling deformation and peel force at which $\eta = 1$ as R_{fc} and F_{wc} respectively, Eq. (6) then gives A_w as

$$A_w = \frac{F_{wc}}{K}\left[\frac{2}{\sqrt{3}}\ln\left(\frac{1}{1-R_{fc}}\right)\right]^{-n} \quad (7)$$

Substituting Eq. (7) into Eq. (6), the weld efficiency is finally given as

$$\eta = \frac{F_w}{F_{wc}} \left[\frac{\ln\left(\frac{1}{1-R_f}\right)}{\ln\left(\frac{1}{1-R_{fc}}\right)} \right]^{-n} \quad (8)$$

3 Results

3.1 Bond Strength and Weld Efficiency

The obtained bond strength of Al/Ti powders/Al strips after CRB depends a lot on thickness reduction and particle contents. As shown in Fig. 5, increasing the thickness reduction and decreasing the Ti particle content improves the bond strength. As indicated by the intercepts of the curves with the horizontal axis in Fig. 5, for a given particle content in low thickness reductions, bonding can not be formed, i.e. the aluminium sheets after the roll bonding are separated with no bonding force. It is also interesting to see from Fig. 5 that increasing the Ti content decreases peel force. The sample without Ti powder has highest value of average peel force, 25 N/mm but it is reduced to 10 N/mm for the sample containing 0.5 wt% Ti powder. Also, adding Ti powders between aluminium sheets lead to increased threshold rolling reduction and the thickness reduction, so that formation of bonding can be begin. It is about 35% and higher than that for aluminium sheets without particles under similar condition. Both observations here indicate that Ti powders between aluminium sheets decreases the bonding achieved in the CRB process of Al.

From conventional tensile testing, the strain-hardening exponent of the Al alloy used has been determined to be $n = 0.221$. Using this value of n, the weld efficiencies calculated from Eq. (8) are shown in Fig. 6. Madaah-Hosseini and Kokabi [26] suggested the η versus R_f relation to be parabolic, and for this reason, best-fitting parabolic curves are also shown in Fig. 6. The data shows that

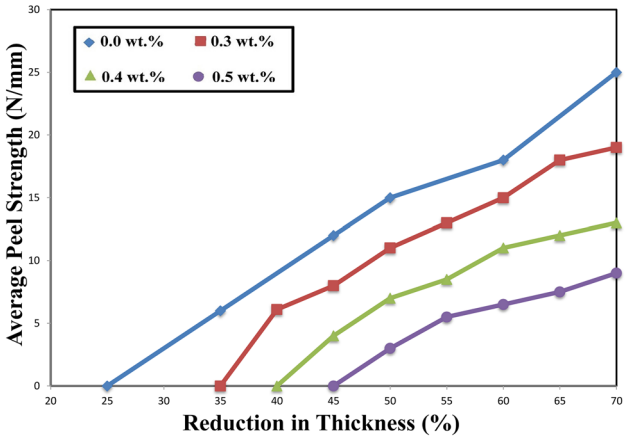

Fig. 5 Changes of peel strength versus Ti powder content and thickness reduction

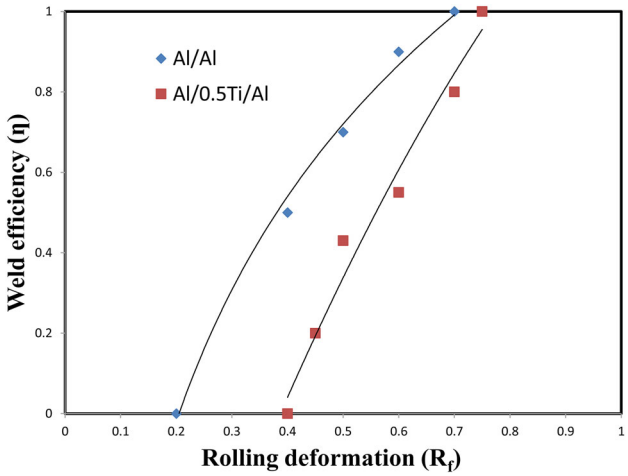

Fig. 6 Variation of weld efficiency of Al strips versus rolling deformation with and without Ti particles

high weld efficiencies approaching unity can be achieved with high rolling reductions. Also, for constant reduction, the weld efficiency in the presence of Ti particles is lower than that in the absence of Ti particles.

3.2 Fractured Surfaces and Bonded Area

The peeled surfaces of the pure Al strips, without Ti addition, cold-roll bonded by different thickness reductions are shown in Fig. 7. A remarkable feature is the occurrence of "stretch lips" [25] that run approximately normal to the rolling direction RD; see Fig. 8 for an example in a larger magnification. Such stretch lips are locations of ductile fracture during the peeling and hence are places where the two Al strips are well bonded together before the peeling. However, as Fig. 8 shows, an observed lip on the peeled surface is just the tip of a ductile fracture point, and the actual bonded area which is larger can be specified by following of stretch lines down the slope of the lip. Since the stretch lips are nearly unidirectionally perpendicular to the RD, the fraction of the bonded area relative to the total area can be estimated by a line intersection method along the RD:

$$\text{Fraction of Bonded Area} = \frac{\sum \Delta X}{X} \quad (9)$$

where the ΔX's are the widths of the stretch lips obtained from a line of length X drawn randomly along the rolling direction (see Fig. 9). The fraction of bonded area estimated this way for Al/Al and Al/Ti/Al samples is shown in Fig. 10. As shown in Fig. 10, bonded area improves by increasing the thickness reduction. The results here tally well with the increase in peel strength and weld efficiency with rolling reductions in Figs. 5 and 6.

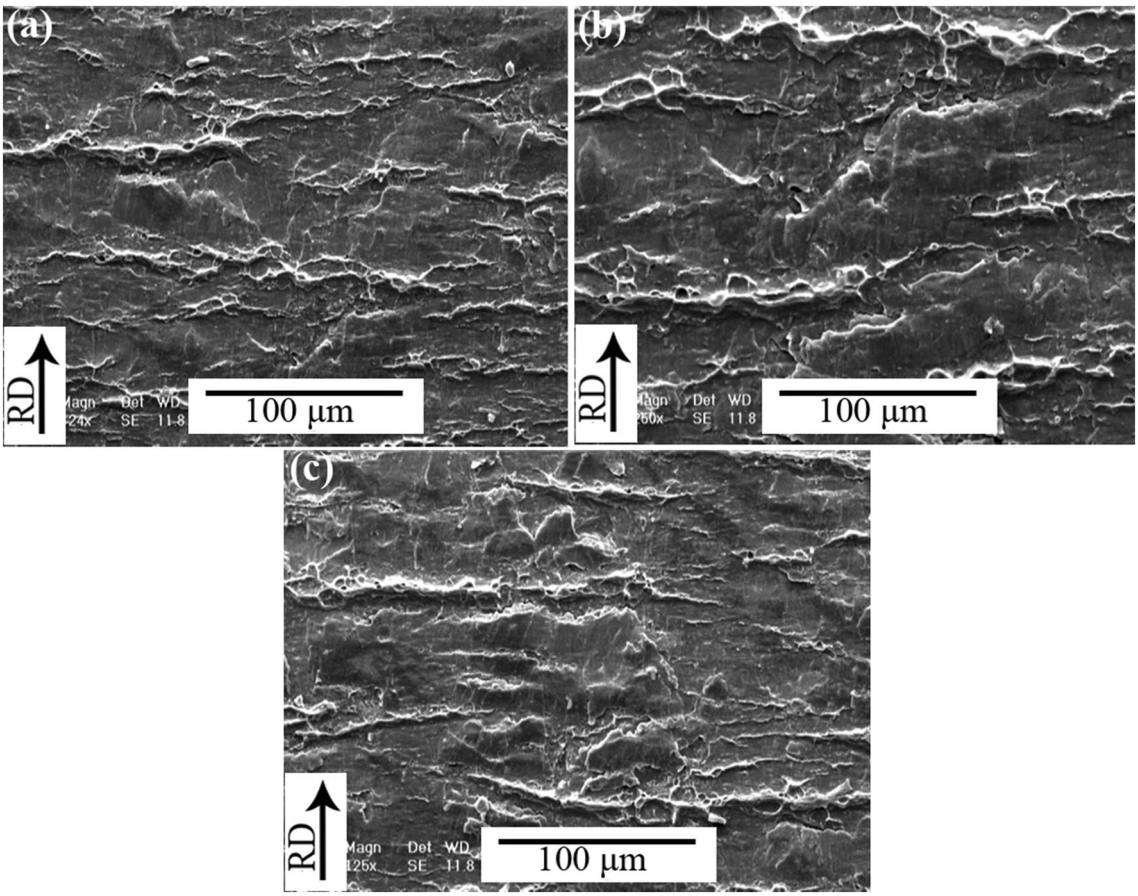

Fig. 7 The peeled surface of cold roll bonded aluminium sheets for different thickness reduction: **a** 50%, **b** 60% and **c** 70%

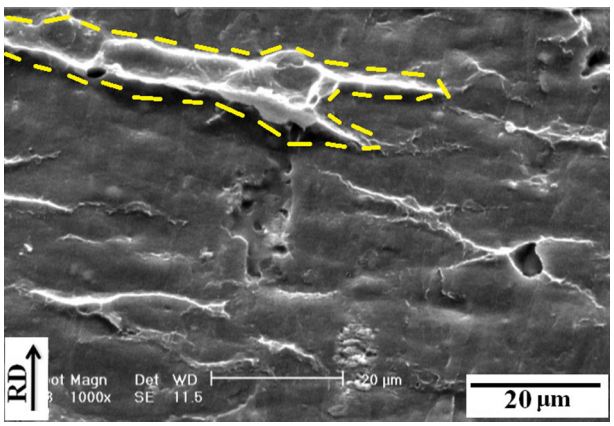

Fig. 8 A "stretch lip" on surface of Al bonded sample after peeling test with R = 50%. The original bonded area is estimated to be the region as marked

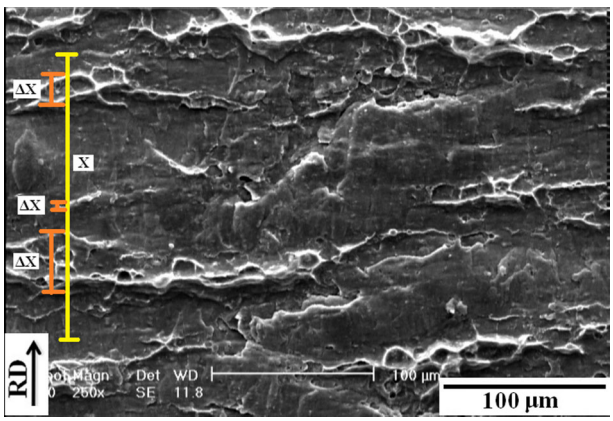

Fig. 9 The fracture surface of roll bonded Al/Al with R = 50%, showing a simplified method for measuring the fraction of bonded surface area via directional stretch lips

Figure 11 shows the longitudinal cross-section of the Al strips with 0.3 and 0.5 wt% Ti addition bonded by 50% rolling reduction. The Ti particles are clearly seen to remain at the interface between the two initial Al strips. Figure 12 shows the peeled surfaces of the Al/Ti/Al samples with different amounts of Ti particles cold-roll bonded by 50% thickness reduction. Figure 10 in fact shows that inserting Ti particles leads to reduction of the bonded area at the same rolling reduction, and this agrees with the fall in peel strength and weld efficiency with Ti addition in Figs. 5 and 6.

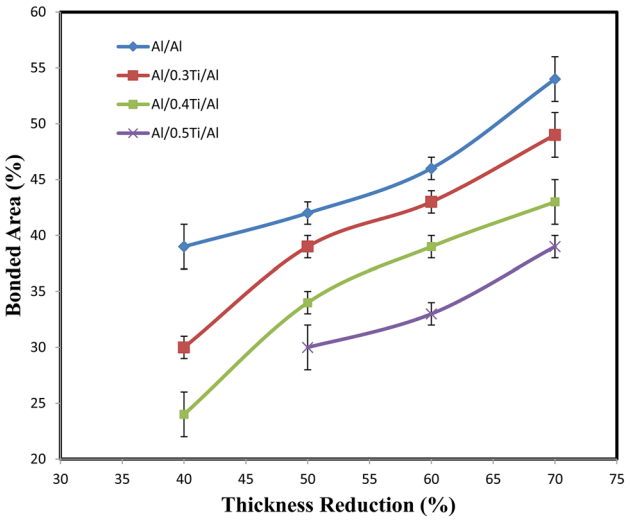

Fig. 10 Bonded area versus rolling reduction for Al/Al and Al/Ti/Al samples

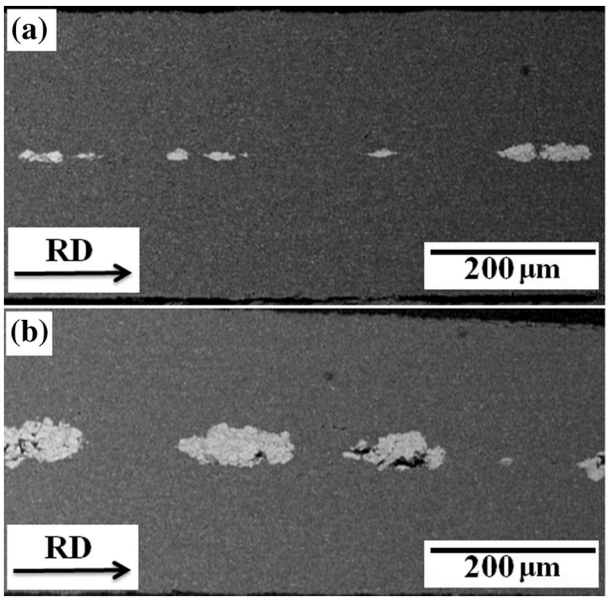

Fig. 11 The cross section of 50% thickness reducted aluminum, with **a** 0.3 wt% and **b** 0.5 wt% Ti particles

4 Discussion

4.1 Bonding Mechanism

As shown in Figs. 5 and 6, for pure Al/Al at least, high peel strength and weld efficiency are achievable under CRB with high enough rolling reductions. The scratch-brushing surface treatment of the Al strips before CRB should remove contaminated layers, and since the rolling process is conducted as soon as practically possible after CRB, re-occurrence of contamination should not be significant. However, for Al surfaces, a layer of oxide passivation film should always exist, and the scratch-brushing surface treatment should also create a deformed rough film.

Therefore, at the beginning of the CRB procedure, fracture of brittle covering oxide layer is expected to take place, and then the underneath metal starts to extrude through the cracks. Then, metallic bond is created from the contact between the virgin metal's asperities of two surfaces [12]. Figure 10 shows that the area of stretch lips or bonded region increases by increasing of thickness reduction. It means more plastic deformation can establish higher virgin metal and then available area for atom-to-atom bonding extends which results in higher weld efficiency. Actually, rolling pressure elevates extruded metal, leading to more bonding areas. According to previous reports, large deformation of materials caused by high rolling pressure in CRB lead to sharing of electrons between two surfaces and bonding at the atomic level [6]. When surface expansion becomes considerably larger, bonding becomes more extensive because of extensive areas of the uncovered base metal while the unbonded regions of hardened surface layers or brittle oxide are confined to only small isolated islands [10, 27–29]. All these explain the increasing peel force, weld efficiency and bonded area with rolling reduction as seen from Figs. 5, 6 and 10.

4.2 Effect of Ti Particles on Bonding

The results in Figs. 5, 6 and 10 show that with increasing content of Ti powders added between Al strips, there is a decrease in bonded area and bond strength. For creating bonding during cold roll bonding, the deformation has to exceed a threshold value, which is the critical (minimum) rolling reduction required to achieve bonding of the strips. In Fig. 5, the threshold deformation for each Ti particle content is the intercept value of the corresponding curve with the horizontal axis, and it is clear that the threshold strain is advanced by increasing the Ti particle amount.

The reasons of such an effect of Ti particles may be two-fold. First, the bonding between the Ti particles and the Al matrix is intrinsically weak; therefore, the presence of more Ti particles only reduces the Al–Al contact and hence weakens the bonding between the two strips. On the peeled surfaces in Fig. 12, stretch lips are clearly visible. From the higher-magnification micrographs in Fig. 12d, f, it is evident that these always occur in the Al matrix between the Ti particles. This indicates that good bonding happens only between the Al matrixes. In fact, certain holes of similar sizes as the surrounding Ti particles are seen on the fractured surfaces of the Al matrix in Fig. 12c–f, and these are most likely the locations into which Ti particles were originally embedded but were pulled out during the peeling. These features therefore indicate that strong bonding

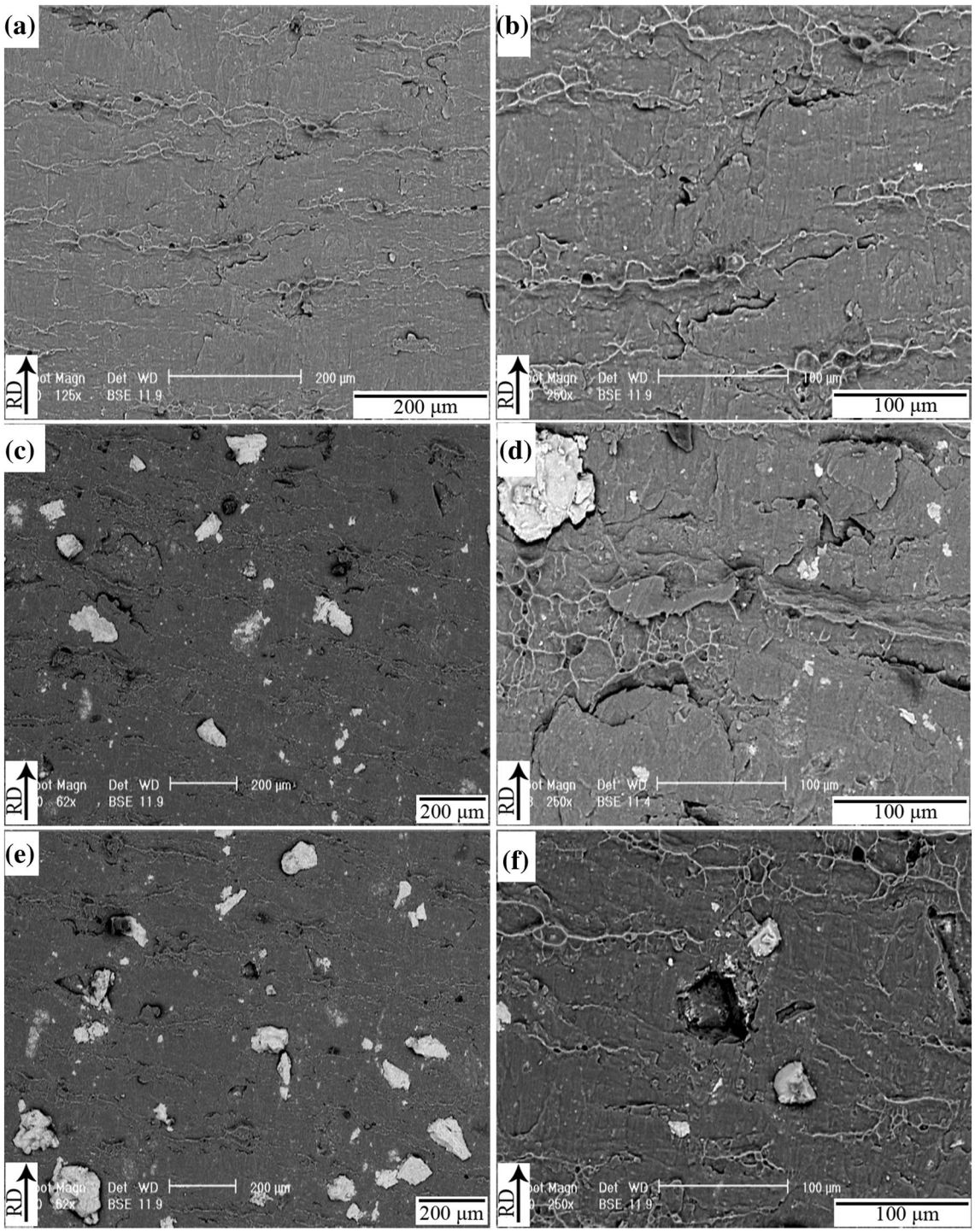

Fig. 12 The peeled surface of Al/Ti/Al sheets after 50% thickness reduction, with **a**, **b** 0 wt%, **c**, **d** 0.3 wt%, and **e**, **f** 0.5 wt% particles at two magnifications

between the Ti particles and the Al could not be established during the CRB process. Therefore the presence of more Ti particles only displaces more area on the Al surfaces for bond formation. This indicates that the bonded area decreases by increasing the Ti content at the same rolling reduction as seen from Fig. 10.

Secondly, it has also been suggested that powder particles can reduce the friction coefficient at a sliding interface because of probable lubrication property [30]. The decreased friction coefficient can be related to the presence of adhesive Ti oxide film on particles. It is hard to break the oxide film on particles as compared to one on the

aluminum sheets [31]. By reduction of the friction coefficient at the interface, the bonding area and as a result the bond strength is decreased [32].

By comparing Fig. 12a and e, it can be seen that, Al/Al laminated surfaces have more extruded metal and more bonding area comparing to the Al/Ti/Al sheets processed under same conditions. On the other hand, to form bonding during roll bonding, it is necessary to overcome the activation energy that is needed for bond formation [33]. With reduction in friction coefficient, it will be more difficult to overcome the activation energy.

5 Conclusions

In this research, bond strength, threshold deformation and weld efficiency of the cold roll bonded Al strips with and without Ti particles were examined and compared. The conclusions can be listed as below:

1. For Al/Al strips with and without Ti particles, an increase in thickness reduction causes an improvement in peeling force and therefore bond strength. It is due to increase in stretch lips areas and therefore plastic deformation.
2. The bond strength, weld efficiency and bonded area decreases by adding Ti powder particles at interface. The Ti particles likely prohibit extrusion, contact and therefore bonding of virgin metals.
3. The threshold deformation of aluminum strips in the absence of Ti particles is about 25%, while this is 35, 40 and 45% for strips containing 0.3, 0.4 and 0.5 wt% Ti particles, respectively. In other words, the bond strength between strips decreases with an increase in the amount of Ti particles.

References

1. Pan D, Gao K, and Yu J, *Mater Sci Technol* **5** (1989) 934.
2. Lukaschkin N D, Borissow A P, and Elrikh A I, *J Mater Proc Technol* **66** (1997) 246.
3. Wu H Y, Lee S, and Wang J Y, *J Mater Proc Technol* **75** (1998) 173.
4. Manesh H D and Taheri A K, *J Mater Sci Technol* **20** (2004) 1064.
5. Le H R, Stucliffe M P F, Wang P Z, Burstein G T, *Acta Mater* **52** (2004) 911.
6. Bay N, *Metal Construct* **18** (1986) 486.
7. Topic I, Höppel H W, and Göken M, *Int J Mater Res* **98** (2007) 320.
8. Vaidyanath L R, and Milner D R, *Br Weld J* **7** (1960) 1.
9. Vaidyanath L R, Nicholas M G, and Milner D R, *Br Weld J* **6** (1959) 13.
10. Wright P K, Snow D A, and Tay C K, *Met Technol* **5** (1978) 24.
11. Mohamed H A, and Washburn J, *Weld J* **30** (1975) 2.
12. Cave J A, and Williams J D, *J Inst Met (Lond)* **101** (1973) 203.
13. Zhang W, and Bay N, *Weld J* **32** (1997) 417s.
14. Zhang W, Bay N, and Wanheim T, *CIRP Ann Manuf Technol* **41** (1992) 293.
15. Sherwood W C, and Milner D R, *J Jpn Inst Met* **97** (1969) 1.
16. McEwan K J B, and Miller D R, *Br Weld J* (1962) 406.
17. Eizadjou M, Manesh H D, and Janghorban K, *Mater Des* **29** (2008) 909.
18. Manesh H D, and Taheri A K, *Mater Des* **24** (2003) 617.
19. Butlin J, and Mackay C A, *Sheet Metal Ind* (1979) 1063.
20. Alizadeh M and Paydar M H, *Mater Des* **30** (2009) 82.
21. Lu C, Tieu K, and Wexler D, *J Mater Process Technol* **209** (2009) 4830.
22. Jia N, Zhu M W, Zheng Y R, He T, and Zhao X, *Acta Metall Sin Eng Lett* **28** (2015) 600.
23. Yazdani Z, Toroghinejad M R, Edris H, Ngan A H W, *J Alloys Compd* **747** (2018) 217.
24. Jamaati R, and Toroghinejad M R, *J Mater Eng Perform* **20** (2011) 191.
25. Yan H, and Lenard J, *Mater Sci Eng A* **385** (2004) 419.
26. Madaah-Hosseini H R, and Kokabi A H, *Mater Sci Eng A* **A335** (2002) 186.
27. Soltani M A, Jamaati R, and Toroghinejad M R, *Mater Sci Eng A* **550** (2012) 367.
28. Bay N, *Met Constr* **18** (1986) 486.
29. Li L, Nagai K, and Yin F, *Sci Technol Adv Mater* **9** (2008) 11.
30. Strijbos S, *Ceramurgia Int* **6** (1980) 119.
31. Chaudhari G P, and Acoff V, *Compos Sci Technol* **69** (2009) 1667.
32. Tzou G Y, Tieu A K, Huang M N, Lin C Y, and We E Y, *J Mater Process Technol* **125** (2002) 664.
33. Yong J, Dashu P, Dong L, and Luoxing L, *J Mater Process Technol* **105** (2000) 32.